Neurod2/6 transcription factors control basal progenitor differentiation and sequential production of neocortical cell subtypes

Kuo Yan[1], Andrew G Newman[1], Svetlana Tutukova[1,2], Maria Gavrish[2], Ingo Bormuth[1], Olga Bormuth[1], Victor Tarabykin[1,2]

1. *Institute of Cell Biology and Neurobiology, Charité – Universitätsmedizin Berlin, Germany*
2. *Institute of Neuroscience, Lobachevsky State University of Nizhny Novgorod, Russia*

Corresponding Author: Victor Tarabykin, victor.tarabykin@charite.de

Abstract

Neurod2 and Neurod6 (Neurod2/6) are key transcription factors that promote neuronal differentiation, however, their role in the developing neocortex is not fully understood. Both genes have similar expression patterns during development as well as binding motifs. In order to investigate their role in cortical neurogenesis, we generated a mouse model deficient for both Neurod2/6. Here we demonstrate that differentiation of Tbr2-positive (Tbr2+) basal progenitors (BPs), but not Pax6+ apical progenitors, was severely defected, resulting in ectopically expanded BPs in perinatal Neurod2/6 deficient brains. The sequential fate specification of cortical neurons was also impaired in the absence of Neurod2/6. Ectopic Tbr2+ BPs expressed multiple proliferation markers and were able to self-renew. Olig2+ glial precursors were consequently over-produced in Neurod2/6 deficient brains. Restoration of Neurod2/6 in the double deficient brains downregulated Tbr2 expression, and exhibited substantial rescue effects on defected laminar subtype specification and excessive gliogenesis. Our work indicates that Neurod2/6 regulate BP differentiation and sequential production of cortical cell subtypes via inhibiting Tbr2-dependent genetic program.

Keywords: Neurod2/6; Tbr2; Olig2; basal progenitor differentiation; Cortical subtype specification

Introduction

During development of the cerebral cortex, all projection neurons originate from neural progenitor cells proliferating in the ventricular and subventricular zones (VZ and SVZ) of the dorsal telencephalon (Subramanian et al., 2017). In the beginning of corticogenesis, this proliferative compartment is a single-layered VZ, with all progenitors contacting the lateral ventricle lumen (Meyer et al., 2000; Homem et al., 2015; Montiel et al., 2016). With development, VZ progenitors elongate their basal process and thereby transform into radial glia cells (RGCs), which play a dual role in development (Malatesta et al., 2003). Like neuroepithelial cells, RGCs function as neuronal progenitors, which are also called apical progenitors (APs) as their cell bodies are lining at the apical surface of neocortex. Additionally, they guide neuronal migration by providing a scaffold for radially migrating neurons through their long basal processes (Rakic, 1972; Levitt and Rakic, 1980).

At the onset of neurogenesis (around E10.5 in mice), some APs undergo asymmetric division and translocate to the basal border of VZ, forming the SVZ. These cells in SVZ are mitotically active, called basal progenitors (BPs), or intermediate progenitors (Noctor et al., 2004 and 2008; Homem et al., 2015; Montiel et al., 2016; Wilsch-Bräuninger et al., 2016). BPs may either generate neurons in one neurogenic division or renew themselves by proliferative mitoses to enrich the neural progenitor pool in SVZ (Noctor et al., 2004; Sessa et al., 2008). SVZ is a critical epicenter for newborn neurons, where they begin to differentiate, extend axons, and start radial migration along radial glia fibers (Bayer and Altman, 1990). SVZ is one of the hotspots in the evolution of the neocortex. It is relatively small in nonplacental mammals and rodents, and comparable in size with that of the VZ. SVZ size increases proportionally to the increment of the neocortex thickness in primates and humans, and significantly overtakes the size of VZ. Respectively, the proportion of proliferating cells in the SVZ of primates is higher than in the VZ.

Tbr2 is a transcription factor (TF) expressed in the SVZ to control BP genesis and proliferation ability. Tbr2 over-expression converts APs to BPs, and prevents BP cell cycle withdrawal (Sessa et al., 2008 and 2017), but it is not known what molecular cascades inactivate Tbr2 in order to initiate pyramidal neuron differentiation. Two members of NeuroD family TFs (Neurod2/6) are potential candidates for this role as their expression arises at the basal border of SVZ where newborn neurons exit cell cycles. While Tbr2 expression vanishes in neurons leaving the SVZ, Neurod2/6 expression is immediately onset in migrating and postmigratory neurons (Wu et al., 2005; Bormuth et al., 2013).

In this work, we investigated the role of NeuroD family TFs in neocortical differentiation and cell fate specification. As both genes have very similar expression patterns and similar targets sets (Bormuth et al., 2013), we inactivated both of them to avoid functional redundancy. This resulted in severe disruption of neocortical differentiation and caused excessive production of Tbr2-positive (Tbr2+) BPs. Additionally, cortical cell subtype specification was also disrupted in the absence of Neurod2/6. Our data indicate that NeuroD2/6 control onset of neuronal differentiation by suppressing Tbr2-dependent transcription program.

Materials and Methods

Mice. The transgenic mice (Neurod6-Cre and Neurod2-Null) and genotyping methodology used in this study were previously described (Goebbels et al., 2006; Bormuth et al., 2013; Yan et al., 2023). The Neurod2/6 double deficient (DKO) mice we used in this report are Neurod2$^{NeoR/NeoR}$; Neurod6$^{Cre/Cre}$, while the control mice are Neurod2$^{Wt/NeoR}$; Neurod6$^{Cre/Cre}$. Generation of NeuroD2/6 DKO mice/embryos: a male and a female control mouse were bred to produce a litter of mixed genotypes (25% incidence of NeuroD2/6 mice/embryos, while 50% incidence of controls). The day of plug discovery was termed as embryonic day 0.5 (E0.5). Male and female embryos were not discriminated in this study. All animal experiments conform to German regulatory standards, and were approved/licensed by the local responsible authority (Landesamt für Gesundheit und Soziales Berlin, LaGeSo, Berlin).

***In utero* electroporation (IUE) and constructs.** IUE was performed as previously described (Yan et al., 2023). Briefly, the anesthetized pregnant mice were kept laid down on a heating pad with constant inhalation of isoflurane (mixed with oxygen). The subcutaneous administration of pain killers (such as temgesic) was applied before a surgery started. An incision of ~15mm was made on the fur and skin along the abdomen midline after cleaned by 70% ethanol. The plasmids (1 µg/µl, mixed with fast green dye 1:20, 000) were loaded in a fine glass capillary and enforced by a vacuum pico-pump into either of the cerebral lateral ventricles. Electrodes were positioned biauricular (anode at the side of injection). Electrodes were positioned biauricular (anode at the side of injection). Electroporation was achieved by an electroporator (CUY21, Sonidel) with setup: 6 times pulses, 35 V voltage, 50 ms pulse duration and 1 sec interval time. The mice on surgeries were monitored every day as for their

health till being sacrificed. Our lab generated a Cre-dependent conditionally bicistronic expression vector (pCAG-FPF-GFP) (Parthasarathy et al., 2014; Yan et al., 2023), which the open reading frames (ORFs) of targeted genes (such as Neurod2 and Neurod6) with their original Kozak sequences were subcloned into for IUE experiments. Tbr2 ORF was subcloned into a constitutive expression vector (pCAGIG, Addgene #11159) for over-expression by IUE. All cloned genes were verified by sequencing. Cloning primers are listed in Tab. S1.

Immunofluorescence (IF). *Day One*: the brain cryo-sections (16 μm in thickness) were post-fixed in 4% paraformaldehyde (PFA, dissolved in 1x PBS) for 15 min followed by twice washes in 1x PBS (10 min each, the same below or otherwise indicated). Subsequently, the sections were incubated in blocking solution (BS, 1x PBS containing 0.5% Triton X-100, 2% BSA and 10% horse serum) at room temperature (RT) for 1 hour, followed by primary antibodies in BS at 4°C over night (O/N). *Day Two*: the sections were first washed 3 times in 1x PBS and then incubated with secondary antibodies in BS for 1.5 hours. After additional 3 times washes in 1x PBS, the slides were mounted in DAKO anti-artifact medium. As for some antibodies that require antigen unmasking (like BrdU antibody), the sections were immerged in unmasking solution (VectorLabs, H-3300) and constantly heated for 10 min by microwave before blocking on *Day One*, followed by cooling to RT. All primary antibodies used in this study are listed in Tab. S2. Fluorescent secondary antibodies are all from Jackson ImmunoResearch (all were raised in donkey, reconstituted according to manual, and diluted 1:500 in use).

I*n situ* hybridization (ISH). ISH was performed as previously reported (Bormuth et al., 2013; Yan et al., 2023). Briefly, *Day One*: the brain cryo-sections were dried in vacuum for 30 min and fixed in 4% PFA dissolved in DEPC-treated 1x PBS (DPBS) for 15 min followed by twice washes in DPBS. Subsequently, the sections were incubated in proteinase K solution (20 mM Tris pH7.5, 1 mM EDTA pH8.0, 20 μg/ml proteinase K) for 2.5 min followed by one wash in DPBS containing 0.2% glycine. The sections were then post-fixed in 4% PFA containing 0.2% glutaraldehyde in DPBS for 15 min followed by twice washes in DPBS, pre-hybridized in hybridization buffer (HB, 50% deionized formamide, 5x SSC, 1% blocking reagent (Roche, 11096176001), 5 mM EDTA, 0.1% Tween20, 0.1% CHAPS, 0.1 mg/ml Heparin, 100 μg/ml yeast RNA) at 65°C for 2 hours, and eventually hybridized with the denatured probes (the probes were heated at 90°C for 5 min before use) at 68°C O/N. *Day Two*: the sections were washed once in 2x SSC pH4.5, and then incubated in RNase solution (0.5 M NaCl, 10 mM Tris pH8.0, 20 μg/ml RNase A) for 30 min at 37°C.

113 Subsequently, the sections were washed stringently 3 times in 50% formamide/2x SSC pH4.5 (30
114 min each) at 63°C, followed by 3 times washes in KTBT buffer (50 mM Tris pH7.5, 150 mM NaCl,
115 10 mM KCl, 1% Triton X-100) at RT. Then the tissues were blocked in ISH BS (KTBT containing
116 20% sheep serum) for 2 hours, followed by incubation with anti-digoxigenin antibody (alkaline
117 phosphatase (AP)-conjugated, Roche, 1:1500) in BS at 4°C O/N. *Day Three*: the sections were
118 washed 4 times in KTBT (30 min each), washed twice in NTMT buffer (100 mM Tris pH9.5,
119 100 mM NaCl, 50 mM $MgCl_2$, 0.1% Tween20), and were eventually incubated in NTMT
120 containing NBT/BCIP (1:50, AP substrates, Roche). The staining was monitored hourly until the
121 signals showed up. The stained sections were subject to an ascending alcohol series (50% - 100%),
122 incubated in clearing solution (benzyl alcohol:benzyl benzoate = 1:2) for 5 min, and finally
123 mounted in Permount mounting media (Thermo Fisher Scientific). All home-made solutions used
124 on *Day One* were DEPC-treated. Primers used for generation of targeted ISH probes are listed in
125 Tab. S1.

126 **Bromodeoxyuridine (BrdU) pulse chase.** 300 µl BrdU solution (10 mg/ml BrdU dissolved in
127 1xPBS) was injected intraperitoneally into a mouse with a sterile needle. The time points and
128 embryonic stages (E12.5 – E17.5) of injections were labelled for each mouse. The injection and
129 sacrifice time points at various stages were tightly controlled (± 0.5 hour). The mouse brains
130 carrying BrdU incorporation were dissected and fixed in 4% PFA either 24 hours later (cell cycle
131 exit analysis) or at P0 (Tbr2+ cell birthdating analysis). The antigen exposure of BrdU during IF
132 was achieved by constant heating as mentioned in IF.

133 **Neurite branchy analysis.** The cortical cells labeled by electroporated membrane-anchored GFP
134 (or bicistronic Tbr2-GFP) were imaged using Leica SL confocal microscope (63x magnification, 2x
135 zoom, 1 µm spaced z-stacks). The neurite complexity of imaged cells was quantified by Sholl
136 analysis (soma as centroid) using the Neuroanatomy plugin of ImageJ (Fiji)**.**

137 **Statistics.** Cell number or ratio quantifications between control and DKO brains were analyzed with
138 two-tailed *Student's* t-test. The statistics for dynamic ratios of Tbr2/BrdU double positive cells relative
139 to all BrdU+ cells (Fig. 2E) was analyzed with two-way *Anova* test. The values for Sholl analysis of
140 neurite arborization (Fig. S7) was analyzed by normality and lognormality test by Prism (Milosević,
141 2007). Values of GFP+ neurons follow (n = 30) normal distribution ($p = 0.024$) and values of Tbr2-
142 expressing neurons (n = 25) is close to normal distribution ($p = 0.074$). The statistics of Sholl analysis

was analyzed with unpaired t- test. Bar charts present mean values ± standard deviation (SD). Significance: p<0.0001, ****; p<0.001, ***; p<0.01, **; p<0.05, *; p>=0.05, ns.

Results

Neurod2/6 deficiency causes expansion of Tbr2+ basal progenitors

Previously we reported the defect of axon growth and agenesis of corpus callosum in Neurod2/6 double deficient (DKO) mice (Bormuth et al., 2013; Yan et al., 2023). We also noticed that simultaneous inactivation of Neurod2 and Neurod6 in the developing neocortex caused anomalies in numbers and positioning of neocortical neurons (Bormuth et al., 2013). In order to investigate potential roles of Neurod2/6 genes in cell fate specification and differentiation, we analyzed the neocortical progenitor cohorts. We first asked if basal progenitors (BPs) are affected when Neurod2/6 are deleted. We thus performed *in situ* hybridization (ISH) and immunofluorescence (IF) for Tbr2, the major BP determinant (Arnold et al., 2008; Sessa et al., 2008), at different stages of corticogenesis. Strikingly, we found progressive accumulation of Tbr2+ BPs in the SVZ and intermediate zone (IZ) of developing DKO brains (Fig. 1A): the number of Tbr2+ BPs in DKO brains is similar with that of controls at E13.5 but significantly increased by 15.92% ± 8.49% at E15.5 ($p = 0.029$, *), and almost triple of the number of BPs in controls perinatally ($p = 0.0023$, **) (Fig. 1B). Consistently, the expression of BP marker genes, such as Scrt2, Svet1 and Brn1 (Paul et al., 2014; Tarabykin et al., 2001; Sugitani et al., 2002), was also expanded in the SVZ/IZ of DKO brains (Fig. S1).

In order to further study the origin of excessive Tbr2+ BPs in DKO brains, we carried out BrdU chase analysis. Pregnant mice were injected with thymidine analog BrdU at serial stages of cortical development (every 24 hours from E12.5 to E17.5). BrdU/Tbr2 colocalization in the neocortex was tested at P0 (Fig. 1C). In such experiments, BrdU will be incorporated into the cells in S phase at the time of injection. On the other hand, cells that contain high levels of BrdU at P0, are the cells that exited mitotic cycle shortly after BrdU injection. The ratios of Tbr2/BrdU double positive (Tbr2+/BrdU+) cells relative to all Tbr2+ BPs indicate that the majority of ectopic Tbr2+ BPs in DKO brains were born after E14.5 (Fig. 1D). Moreover, we quantified the ratios of Tbr2+/BrdU+ cells born from E12.5 till E17.5 relative to all BrdU+ cells at P0. This number reflects the fraction of cells that left mitotic cycle at a defined stage of corticogenesis that maintained Tbr2 expression at P0. In control brains, a

very small fraction (less than 5%) of cells that were born at E12.5 still retained Tbr2 and were located in the SVZ/IZ. In DKO brains, such a fraction was almost doubled. This trend was also observed for the newly born cells at every tested stage of development (Fig. 1E). These data indicate that inactivation of Neurod2/6 in the developing neocortex causes arrest of neuronal differentiation, retention of postmitotic cells in the SVZ/IZ and inability to inactivate Tbr2-dependent genetic program.

Next we asked whether Neurod2/6 deficiency could influence cell cycle exit and onset of neuronal differentiation. Here we utilized 24 h BrdU chase. In these experiments, BrdU was injected at four stages: E12.5 till E15.5. The proportions of progenitors quitting cell cycles after one day were counted as the numbers of BrdU+/Ki67- cells relative to total BrdU+ cell numbers (Fig. 1F). The progenitor proportions exiting cell cycle in DKO cortices are similar with those of controls at E12.5 ($p = 0.62$, ns) and E13.5 ($p = 0.87$, ns), however, the proportions were significantly decreased in DKO brains in comparison to those of control brains at E14.5 (by 14.48% ± 5.10%; $p = 0.018$, *) and E15.5 (by 19.55% ± 7.11%; $p = 0.021$, *) (Fig. 1G). As Neurod2/6 are expressed in Tbr2+ BPs but not in Pax6+ apical progenitors (see below), these data indicate that it is a fraction of Tbr2+ cells that retain cycling in DKO brains.

Neocortical cell type specification is disrupted in Neurod2/6 deficient mice

We reasoned if Neurod2/6 deficiency causes such a dramatic change in the cortical differentiation program, so that many cortical cells retain Tbr2 expression and do not commence radial migration, it might cause alterations in neocortical cytoarchitecture. We quantified the proportions of different cell types in the developing neocortex. We found that the proportion of Satb2+ upper layer (UL) neurons was increased by 25.11% ± 7.18% ($p = 0.0081$, **) while the proportion of Ctip2+ deeper layer (DL) neurons was decreased by 38.20% ± 6.89% ($p = 0.00050$, ***) in DKO brains compared with control brains at E15.5. Satb2 is an UL neuron specifying TF that acts by suppressing Ctip2 expression (Britanova et al., 2006 and 2008). However, there are a subset of transient Satb2+/Ctip2+ neurons in the developing neocortex. The number of such Satb2+/Ctip2+ cells was almost doubled in DKO brains ($p = 0.026$, *) (Fig. 2A, B). IF for other layer specific markers such as Brn2 (UL, Dominguez., et al., 2013; Sugitani et al., 2002) and Tbr1 (DL, Hevner et al., 2001) at E15.5 confirmed the shift in cell fate specification (Fig. 2C). It turned out that the proportion of Brn2+ UL neurons was significantly increased by 27.17% ± 10.35% ($p = 0.030$, *) while the proportion of Tbr1+ DL neurons was decreased by 29.50% ± 7.39% ($p = 0.0040$, **) in the cortical plate (CP) of DKO brains (Fig. 2D, 2E). Additionally, IF for Oct6 (UL marker, Dominguez., et al., 2013) and Sox5 (DL marker, Kwan et al.,

2008) further strengthened our findings (Fig. S2A). These data indicate that Neurod2/6 deficiency causes expansion of UL neurons at expense of DL neurons during early cortical development.

However, at later stages of development not only the number of DL neurons was reduced relative to the controls, but also does the number of UL neurons. IF for Satb2 and Ctip2 demonstrated that UL and DL neurons were both reduced in DKO brains perinatally. Satb2+ UL and Ctip2+ DL neurons were decreased by 15.61% ± 11.07% ($p = 0.041$, *) and by 21.31% ± 17.17% ($p = 0.00080$, ***) in DKO brains, respectively, compared with controls (Fig. 2F). Likewise, Brn2+ UL and Tbr1+ DL cells were decreased by 16.82% ± 5.78% ($p = 0.011$, *) and by 38.68% ± 22.64% ($p < 0.0001$, ****), respectively, in DKO brains at P0 (Fig. 2G). IF for other layer markers, such as Oct6, Foxp2 (DL marker, Kast et al., 2019) and Sox5, confirmed these findings (Fig. S2B, S2C). Our data indicate that Neurod2/6 control the specification of neocortical subtypes of projection neurons.

Neurod2/6 deficiency does not affect Pax6+ apical progenitors

Cortical laminar subtype specification is coordinated with their molecular expression profile, which has been largely programmed in the dividing progenitors (Molyneaux et al., 2007; Telley et al., 2016; Oberst et al., 2019). Hence we investigated if APs are also affected in the neocortex of Neurod2/6 DKO mice. The expression of Pax6, the AP marker and cell identity determinant in the VZ (Götz et al., 1998), was not changed in DKO cortices as compared to the control brains throughout embryonic neurogenesis (Fig. S3A). Another landmark of cell fate specification is an expression gradient of phosphorylated Erk1/2 (pErk1/2) in the developing neocortex. It is essential for neuronal differentiation of APs and laminar specification (Ortega et al., 2010; Xing et al., 2016; Gantner et al., 2021; Parthasarathy et al., 2021). The graded expression of pErk1/2 was not altered in DKO brains (Fig. S3B). In addition, we analyzed if Neurod2/6 regulate the expression of genes that are involved in the control of cortical area specification in the VZ (O'Leary et al., 2007; Caronia-Brown et al., 2014). Neither lateral high to medial low gradients of expression of area regulators, such as Coup-TF and Pax6 (Fig. S4A-A' and S4B-B'), nor medial high to lateral low graded regulators, such as Etv5 and Emx1 (Fig. S4C-C' and S4D-D'), were changed in DKO cortices as compared to the control brains. Taken together, our data indicate that Neurod2/6 are not involved in direct regulation of APs.

Neurod2/6 regulate basal progenitor differentiation and laminar fate specification cell-autonomously

The NeuroD members are key TFs that facilitate neuronal maturation and axonal navigation cell-autonomously (Tutukova et al., 2021; Pieper et al., 2019; Yan et al., 2023). Therefore, we asked if

233 Neurod2/6 also regulate BP differentiation and cell fate specification in a cell-autonomous manner.
234 In order to address this, we first analyzed the expression of Neurod2 or Cre (that recapitulates Neu-
235 rod6 expression in NeuroD6^{Cre} mouse line) in APs and BPs. Both Neurod2 and Cre display mutually
236 exclusive expression patterns with Pax6 (Fig. 3A, 3C). However, Neurod2 and Cre have been found
237 to colocalize with Tbr2 in a subpopulation of BPs throughout neurogenesis at the border between BPs
238 and newborn neurons starting from E11.5 (Fig. 3B, 3D). Notably, the cells co-expressing Cre/Tbr2
239 are progressively increasing in Neurod2/6 DKO cortex, implicating that Tbr2+ ectopic cells in DKO
240 brains are indeed those that fail to differentiate and migrate due to intrinsic deficiency of Neurod2/6
241 (Fig. 3D). Extrinsic factors, such as radial glia fibers and Reelin, in cerebral cortex are known to be
242 essential for proper positioning of newborn neurons (Tissir et al., *review*, 2003; Rakic, *review*, 2009;
243 Belvindrah et al., 2007; Liu et al., 2015). In order to test if these can be changed in DKO brains, we
244 performed IF for – Nestin, Blbp (brain lipid binding protein) (Kriegstein et al., 2003; Anthony et al.,
245 2005), and Reelin. We found radial glia scaffold as well as Reelin expression to be normal throughout
246 corticogenesis in DKO brains (Fig. S5).

247 We next performed *in utero* electroporation (IUE) with the constructs that enable Cre-dependent ex-
248 pression of either GFP or bicistronic Neurod6-GFP at E12.5 and analyzed the brains at E15.5. While
249 IUE of GFP into control and DKO brains did not disturb the expression of Tbr2 (Fig. 4A) or Pax6
250 (Fig. S6A), enforced Neurod6 expression caused depletion of Tbr2+ BPs (Fig. 4B), but not Pax6+
251 APs (Fig. S6B). In line with this, ISH for Tbr2 on Neurod6 electroporated brains displayed downreg-
252 ulation of Tbr2 expression at electroporation sites, but not in the neighboring areas (Fig. S6C). In
253 order to test if Neurod6 restoration in DKO brains can rescue the defects of cell fate specification, we
254 performed co-IF for GFP and laminar markers on the electroporated brains. We found that the pro-
255 portion of GFP+/Satb2+ cells in GFP-electroporated DKO brains (~77.90%) was much higher than
256 that in GFP-electroporated control brains (~52.11%), whereas the proportion of GFP+/Ctip2+ cells
257 in GFP-electroporated DKO brains (~46.44%) was lower than that in control brains (~56.62%), mim-
258 icking the similar deficits of laminar fate decision in DKO brains as in Fig 2A – 2E. IUE of Neurod6
259 into DKO brains reinstated the normal proportions of Satb2+ or Ctip2+ cells (GFP+/Satb2+: ~56.65%
260 and GFP+/Ctip2+: ~59.32%) comparable to those in GFP-electroporated controls (Fig. 4C-4E).
261 Moreover, the rescue effects of Neurod6 were further underpinned by the evidence on additional
262 laminar markers, such as Brn2 and Tbr1 (Fig. 4F-4H). Such acute and focal Neurod6 restoration in a

limited subpopulation of progenitors could rescue the cellular deficits in cell fate specification, indicating that Neurod2/6 control cell fate cell-autonomously. Our data also indicate that Neurod2/6 are critical for sequential production of subtypes of neocortical projection neurons.

Neurod2/6 promote timely specification of basal progenitors into upper layer neurons

Though Tbr2+ BPs give rise to neurons in all cortical layers, they mainly produce UL neurons after E14.5 through neurogenic divisions (Sessa et al., 2008; Kowalczyk et al., 2009; Mihalas et al., 2016). However, a large population of BPs in Neurod2/6 DKO cortices retain their Tbr2 expression and are arrested in SVZ/IZ (Fig. 1). We thus reasoned if UL neuron reduction in DKO brains (Fig 2F, 2G) is resulted from failure of Tbr2+ BP differentiation. Tuj1, the earliest neuronal fate marker (Memberg et al., 1995; Reyes et al., 2008), is strongly expressed in postmitotic compartment but minimally in Tbr2+ BPs (Fig. 5A). Enforced Neurod2 expression in both control and DKO brains led to precocious activation of Tuj1 expression in Tbr2+ BPs at the IUE sites, but not those in the neighboring cells (Fig. 5B, 5C), indicating Neurod2/6 expression is sufficient to drive BPs into neurogenic differentiation. To further find out if the ectopic BPs born after E14.5 are properly specified to UL neurons in the presence of Neurod2, we performed IF for GFP and Satb2 to analyze the brains that were electroporated with GFP or bicistronic Neurod2-GFP at E14.5 and collected at E18.5 (Fig. 5D). The proportion of GFP+/Satb2+ cells was ~77.48% in GFP-electroporated control brains but significantly decreased to ~35.18% in Neurod2/6 DKO brains ($p < 0.0001$, ****), largely due to the presence of Satb2 fated cells arrested in the SVZ/IZ. Notably, Neurod2 restoration in DKO brains increased the proportion of GFP+/Satb2+ cells up to the similar level (~75.11%) with that in GFP-electroporated control brains (Fig. 5E).

On the other hand, we studied if excessive Tbr2 expression in BPs affects UL neuron commitment. We electroporated GFP or bicistronic Tbr2-GFP in wild type brains at E14.5 and analyzed the brains at E18.5 (Fig. 5F). Tbr2 over-expression *in vivo* prevented radial migration of cortical projection neurons and impaired their neurite arborization (Fig. S7), highly consistent with the previous report (Sessa, et al., 2017). Importantly, IUE of bicistronic Tbr2-GFP retained a large population of GFP+/Satb2- cells in the SVZ/IZ and thus led to significantly reduced production of Satb2+ UL cells (by 46.11% ± 6.41%; $p = 0.00040$, ***) in comparison to GFP-electroporated brains (Fig. 5G),

291 resembling the deficits of UL projection neuron specification in Neuod2/6 DKO brains. Taken to-
292 gether, Neurod2/6 are essential for timely specification of Tbr2 BPs into UL neurons at later neuro-
293 genic stages of neocortex.

294 **Olig2+ glial precursors are ectopically upregulated in the cortex of Neurod2/6 deficient mice**

295 Next we reasoned if the ectopic Tbr2+ cells that fail to differentiate into neurons in Neurod2/6 defi-
296 cient brains could retain their proliferating activity. We performed co-IF for Tbr2 and proliferation
297 markers, such as PCNA (proliferating cell nuclear antigen) or Ki67 (Gerdes et al., 1991; Maga et
298 al., 2003; Juríková et al., 2016; Sobecki et al., 2016). We detected substantial numbers of Tbr2+
299 cells, though not all, expressing either PCNA and/or Ki67 in the IZ of DKO brains at P0 (Fig. 6A,
300 6B). Sox2 is a key regulator for self-renewal and proliferation of neural progenitors (Taranova et al.,
301 2006; Hagey et al., 2014; Pagin et al., 2021). IF for Tbr2 and Sox2 detected increase in number of
302 Tbr2+/Sox2+ cells in the IZ of DKO brains as compared with controls (Fig. 6C). Taken together,
303 our data indicate that ectopic Tbr2+ cells in DKO brains, at least in part, retain their proliferating
304 activity.
305 Delay in the mitotic cycle exit or ectopic progenitor proliferation often causes expansion of cell
306 numbers of later born subtypes (Nieto et al., 2001; Miller et al., 2007; Kohwi et al., 2013). Consid-
307 ering BPs can produce glial lineage following UL neurogenesis (Li, et al., 2021), we therefore hy-
308 pothesized that more proliferative BPs in DKO brains could over-produce glial cells at the late stage
309 of embryonic corticogenesis. To verify this, we performed IF for Cre and Olig2 - a marker for glial
310 precursors and oligodendrocytes (Marshall et al., 2005; Ono et al., 2009; Seuntjens et al., 2009).
311 The number of Olig2+ cells in DKO brains was almost doubled of that in control brains at P0 (p =
312 0.0053, **; Fig. 6D, 6E). Notably, Cre expression (Neurod6-expressing excitatory neurons) never
313 overlapped with Olig2 expression, indicating that Neurod2/6 do not act in Olig2+ cells directly to
314 regulate their cell fate or production. On the other hand, IUE of Neurod6 into the progenitors in
315 DKO brains downregulated the number of Olig2+ cells in the electroporation area to the similar
316 level as that in the GFP-electroporated controls (Fig. 6F, 6G). These data indicate that Neurod2/6-
317 driven genetic program suppresses glial cell fate in BPs and controls a proper timely switch from
318 neurogenesis to gliogenesis.

Discussion

Neurod2/6 expression in cerebral cortex begins with the onset of neurogenesis in the SVZ and retains in the postmitotic neurons (Wu et al., 2005; Goebbels et al., 2006; Bormuth et al., 2013). These TFs have been long known to regulate multiple cellular processes in corticogenesis, such as neuronal differentiation, migration, axon navigation and synapse plasticity (Wu et al., 2005; Ince-Dunn et al., 2006; Bormuth et al., 2013; Guzelsoy et al., 2019; Yan et al., 2023). However, their downstream mechanisms underlying proneural differentiation and their potential role in sequential specification of cortical cell subtypes are poorly studied. One of the aims of this study was to test the hypothesis that Neurod2/6 might control differentiation of specific subtypes of neural progenitors. Indeed we could show that Neurod2/6 do not have a direct role in differentiation of APs, but specifically regulate BP differentiation and thus the cell fates of BPs' progeny.

BPs are derived from Pax6+ APs and populated in the SVZ. They may either produce neurons in one neurogenic division or undergo one or more self-renewing divisions. BPs thus serve as a secondary progenitor pool to amplify neuron production (Noctor et al., 2004; Sessa et al., 2017). However, how a BP cell makes the neurogenic versus proliferative decision is unclear. Our mouse model turned out to be a unique tool to study the mechanisms and effects of endogenous BP expansion. Tbr2 is a signature gene for BPs, and has been reported to be a key TF that facilitates BP genesis and self-renewal, supported by the findings that Tbr2 deletion in forebrain resulted in reduced BP numbers and mitoses, and consequently reduced number of neurons in all cortical layers (Arnold et al., 2008; Sessa et al., 2008). Furthermore, Tbr2 over-expression by IUE increased mitoses in SVZ and inhibited the genes accelerating cell cycle exit, such as Btg2 and Cdkn1b (Arnold et al., 2008; Sessa et al., 2008 and 2017). Consistently, we found that ectopic BPs in DKO brains retained Tbr2 expression and failed to differentiate. These cells instead reentered proliferative cycling. On the other hand, Neurod2/6 were expressed in a subset of BPs throughout cortical neurogenesis and promoted BP cell cycle exit. In addition, acute Neurod2/6 over-expression downregulated Tbr2 expression and converted almost all Neurod2/6+ BPs into neurons. Collectively, these results indicate that Neurod2/6 trigger the immediate neurogenic process in BPs by suppressing Tbr2-dependent proliferative program.

It has been shown that BPs produce cortical neurons of all layers with progressive cell fate restriction (Noctor et al., 2004; Mihalas et al., 2016; Sessa et al., 2017). Early born BPs (E11.5 – E13.5) may be specified either into DL neurons in one round rapid division or into UL neurons due

to self-renewal or protracted differentiation, but late BPs (since E15.5) exclusively produce UL neurons (Mihalas et al., 2016). The same report also indicated that Tbr2 critically regulated this tempo of BP neurogenesis and thus the laminar fates of daughter cells. One of their main findings to support this idea was that Tbr2 deficiency in BPs caused expanded DL neuron production (birthday mainly at E12.5) at the expense of UL neurons. Intriguingly, we showed that Tbr2 upregulation due to Neurod2/6 deficiency exerted an opposite effect on laminar fates to Tbr2 deficiency, and that the deficits in laminar fate choice could be almost completely rescued by Neurod2/6 restoration at E12.5. These data suggest that Neurod2/6 regulate timely acquisition of cortical DL subtypes upstream of Tbr2 during early neurogenesis.

The reduced UL neurons in Tbr2 deficient mouse brains were resulted either from inadequate BP amplification (Arnold et al., 2008; Sessa et al., 2008) or from impaired timely differentiation (Mihalas et al., 2016) during early neurogenesis (E11.5 – E13.5), but Tbr2's roles in late neurogenesis (E15.5 – E17.5) is not thoroughly elucidated. Here we demonstrated Tbr2 IUE at E14.5 prevented progenitors from differentiation into Satb2+ UL neurons. Additionally, others and we showed that Tbr2 electroporation led to impaired radial migration and neurite outgrowth of cortical pyramidal neurons (Sessa et al., 2017 and Fig. S7). These results suggest that Tbr2 over-expression in late neurogenesis may impede UL neuron differentiation and maturation. Notably, Tbr2+ BPs were arrested in SVZ/IZ and unable to differentiate into Satb2+ UL cells in Neurod2/6 DKO brains, but Neurod2/6 restoration at E14.5 completely rescued the defected generation of UL neurons. Neurod2/6 thus facilitate UL neurogenesis by driving BP differentiation after E14.5.

Glia cells arise from the progenitor cells in the VZ/SVZ following UL neuron generation during corticogenesis (Miller et al., 2007). The timing of switch from neurogenesis to gliogenesis in APs is critically regulated by proneural TFs, such as Ngn2 and Mash1. Ngn2/Mash1 double deficiency in APs caused premature and excessive astrogenesis at the expense of their neurogenic capacity (Nieto et al., 2001). BPs have been recently identified as a transient amplification source for Olig2+ glial precursors after E16.5 (Li et al., 2021; Liang et al., 2024). Here we show that deficiency of another group of proneural TFs (Neurod2/6) resulted in ectopic cycling of BPs and thus over-production of Olig2+ precursors. This finding is also supported by the IUE experiments that Neurod2/6 restoration in DKO brains reduced the local numbers of Tbr2+ BPs and Olig2+ glial precursors to a similar level with those of controls. Taken all together, Neurod2/6 govern sequential commitment of cortical subtype fates, such as DL versus UL neurons, neuronal versus glial, via regulating timely differentiation of Tbr2+ BPs.

Notes

We here thank R Wunderlich, R Dannenberg, D Lajkó and J Schüller for excellent technical support. Neurod2-Null (Neurod2$^{NeoR/NeoR}$) and Neurod6-Null (namely NEX-Cre, Neurod6$^{Cre/Cre}$) mice were contributed by T Yonemasu and S Goebbels, respectively, and provided by KA Nave and MH Schwab, Max-Planck-Institute of Experimental Medicine, Göttingen, Germany. This study was financially supported by DFG (grant TA 303/14-1), and by the Russian Science Foundation, project № 21-65-00017 (VT and ST, genetic rescue experiments).

Author contributions

Kuo Yan: 1) conceptualization of the project. 2) writing and editing of manuscript draft. 3) phenotypic characterization of Neurod2/6 mouse model. 4) IUE and investigation of IUE effects on Neurod2/6 mouse model.

Andrew G Newman: 1) data analysis and interpretation

Svetlana Tutukova: 1) Tbr2 IUE and experimental characterization of Tbr2 IUE effects on wt mice.

Maria Gavrish: 1) Sample preparation

Ingo Bormuth and Olga Bormuth: 1) Tbr2 ISH on Neurod2/6 mouse model.

Victor Tarabykin: 1) conceptualization, supervision and administration of the project. 2) writing and editing of manuscript draft. 3) funding acquisition.

References

Altman J, Bayer SA. (1990) **Prolonged sojourn of developing pyramidal cells in the intermediate zone of the hippocampus and their settling in the stratum pyramidale.** *J Comp Neurol.* Nov 15;301(3):343-64.

Anthony TE, Mason HA, Gridley T, Fishell G, Heintz N. (2005) **Brain lipid-binding protein is a direct target of Notch signaling in radial glial cells.** *Genes Dev.* May 1;19(9):1028-33.

405 Arnold SJ, Huang GJ, Cheung AF, Era T, Nishikawa S, Bikoff EK, Molnár Z, Robertson EJ,
406 Groszer M. (2008) **The T-box transcription factor Eomes/Tbr2 regulates neurogenesis**
407 **in the cortical subventricular zone.** *Genes Dev.* Sep 15;22(18):2479-84.
408 Belvindrah R, Graus-Porta D, Goebbels S, Nave KA, Müller U. (2007) **Beta1 integrins in radial**
409 **glia but not in migrating neurons are essential for the formation of cell layers in the**
410 **cerebral cortex.** *J Neurosci*. Dec 12;27(50):13854-65.
411 Bormuth, I., Yan, K., Yonemasu, T., Gummert, M., Zhang, M., Wichert, S., Grishina, O., Pieper, A.,
412 Zhang, W., Goebbels, S., et al. (2013) **Neuronal basic helix-loop-helix proteins Neurod2/6**
413 **regulate cortical commissure formation before midline interactions**. *J. Neurosci.,* 33,
414 641 – 651.
415 Britanova, O., Alifragis, P., Junek, S., Jones, K., Gruss, P., & Tarabykin, V. (2006) **Satb2 is a**
416 **postmitotic determinant for upper-layer neuron specification in the neocortex.** *Dev*
417 *Biol.,* 298 (1):299 – 311.
418 Britanova, O., de Juan Romero, C., Cheung, A., Kwan, K.Y., Schwark, M., Gyorgy, A., Vogel, T.,
419 Akopov, S., Mitkovski, M., Agoston, D., et al. (2008) **Satb2 is a postmitotic determinant**
420 **for upper-layer neuron specification in the neocortex.** *Neuron,* 57, 378 – 392.
421 Caronia-Brown G, Yoshida M, Gulden F, Assimacopoulos S, Grove EA. (2014) **The cortical hem**
422 **regulates the size and patterning of neocortex.** *Development.* Jul;141(14):2855-65.
423 Dominguez MH, Ayoub AE, Rakic P. (2013) **POU-III transcription factors (Brn1, Brn2, and**
424 **Oct6) influence neurogenesis, molecular identity, and migratory destination of upper-**
425 **layer cells of the cerebral cortex.** *Cereb Cortex.* Nov;23(11):2632-43.
426 Gantner CW, Hunt CPJ, Niclis JC, Penna V, McDougall SJ, Thompson LH, Parish CL. (2021)
427 **FGF-MAPK signaling regulates human deep-layer corticogenesis.** *Stem Cell Reports.*
428 May 11;16(5):1262-1275.
429 Gerdes J, Li L, Schlueter C, Duchrow M, Wohlenberg C, Gerlach C, Stahmer I, Kloth S, Brandt E,
430 Flad HD. (1991) **Immunobiochemical and molecular biologic characterization of the**
431 **cell proliferation-associated nuclear antigen that is defined by monoclonal antibody Ki-**
432 **67.** *Am J Pathol.* Apr;138(4):867-73.
433 Goebbels, S., Bormuth, I., Bode, U., Hermanson, O., Schwab, M.H., & Nave, K.-A. (2006) **Genetic**
434 **targeting of principal neurons in neocortex and hippocampus of NEX-Cre mice**. *Genes.*
435 *N. Y. N 2000,* 44, 611 – 621.

436 Götz M, Stoykova A, Gruss P. (1998) **Pax6 controls radial glia differentiation in the cerebral**
437 **cortex.** *Neuron.* Nov;21(5):1031-44.
438 Guzelsoy G, Akkaya C, Atak D, Dunn CD, Kabakcioglu A, Ozlu N, Ince-Dunn G. (2019) **Terminal**
439 **neuron localization to the upper cortical plate is controlled by the transcription factor**
440 **NEUROD2.** *Sci Rep.* Dec 23;9(1):19697.
441 Hagey DW, Muhr J. (2014) **Sox2 acts in a dose-dependent fashion to regulate proliferation of**
442 **cortical progenitors.** *Cell Rep.* Dec 11;9(5):1908-1920.
443 Hevner RF, Shi L, Justice N, Hsueh Y, Sheng M, Smiga S, Bulfone A, Goffinet AM, Campagnoni
444 AT, Rubenstein JL. (2001) **Tbr1 regulates differentiation of the preplate and layer 6.**
445 *Neuron.* Feb;29(2):353-66.
446 Homem CC, Repic M, Knoblich JA. (2015) **Proliferation control in neural stem and progenitor**
447 **cells.** *Nat Rev Neurosci.* Nov;16(11):647-59.
448 Ince-Dunn G, Hall BJ, Hu SC, Ripley B, Huganir RL, Olson JM, Tapscott SJ, Ghosh A. (2006)
449 **Regulation of thalamocortical patterning and synaptic maturation by NeuroD2.** *Neu-*
450 *ron.* Mar 2;49(5):683-95.
451 Juríková M, Danihel Ľ, Polák Š, Varga I. (2016) **Ki67, PCNA, and MCM proteins: Markers of**
452 **proliferation in the diagnosis of breast cancer.** *Acta Histochem*. Jun;118(5):544-52.
453 Kast RJ, Lanjewar AL, Smith CD, Levitt P. (2019) **FOXP2 exhibits projection neuron class spe-**
454 **cific expression, but is not required for multiple aspects of cortical histogenesis.** *Elife.*
455 May 17;8:e42012.
456 Kohwi M, Doe CQ. (2013) **Temporal fate specification and neural progenitor competence dur-**
457 **ing development.** *Nat Rev Neurosci.* Dec;14(12):823-38.
458 Kowalczyk T, Pontious A, Englund C, Daza RA, Bedogni F, Hodge R, Attardo A, Bell C, Huttner
459 WB, Hevner RF. (2009) **Intermediate neuronal progenitors (basal progenitors) produce**
460 **pyramidal-projection neurons for all layers of cerebral cortex.** *Cereb Cortex.*
461 Oct;19(10):2439-50.
462 Kriegstein AR, Götz M. (2003) **Radial glia diversity: a matter of cell fate.** *Glia*. Jul;43(1):37-43.
463 Kwan KY, Lam MM, Krsnik Z, Kawasawa YI, Lefebvre V, Sestan N. (2008) **SOX5 postmitotically**
464 **regulates migration, postmigratory differentiation, and projections of subplate and**
465 **deep-layer neocortical neurons.** *Proc Natl Acad Sci U S A.* Oct 14;105(41):16021-6.

Levitt P, Rakic P. (1980) **Immunoperoxidase localization of glial fibrillary acidic protein in radial glial cells and astrocytes of the developing rhesus monkey brain.** *J Comp Neurol.* Oct 1;193(3):815-40.

Li X, Liu G, Yang L, Li Z, Zhang Z, Xu Z, Cai Y, Du H, Su Z, Wang Z, Duan Y, Chen H, Shang Z, You Y, Zhang Q, He M, Chen B, Yang Z. (2021) **Decoding Cortical Glial Cell Development.** *Neurosci Bull.* Apr;37(4):440-460.

Liang XG, Hoang K, Meyerink BL, Kc P, Paraiso K, Wang L, Jones IR, Zhang Y, Katzman S, Finn TS, Tsyporin J, Qu F, Chen Z, Visel A, Kriegstein A, Shen Y, Pilaz LJ, Chen B. (2024) **A conserved molecular logic for neurogenesis to gliogenesis switch in the cerebral cortex.** *Proc Natl Acad Sci U S A.* May 14;121(20):e2321711121.

Liu R, Yang Y, Shen J, Chen H, Zhang Q, Ba R, Wei Y, Li KC, Zhang X, Zhao C. (2015) **Fstl1 is involved in the regulation of radial glial scaffold development.** *Mol Brain.* Sep 17;8:53.

Maga G, Hubscher U. (2003) **Proliferating cell nuclear antigen (PCNA): a dancer with many partners.** *J Cell Sci.* Aug 1;116(Pt 15):3051-60.

Marshall CA, Novitch BG, Goldman JE. (2005) **Olig2 directs astrocyte and oligodendrocyte formation in postnatal subventricular zone cells.** *J Neurosci.* Aug 10;25(32):7289-98.

Malatesta P, Hack MA, Hartfuss E, Kettenmann H, Klinkert W, Kirchhoff F, Götz M. (2003) **Neuronal or glial progeny: regional differences in radial glia fate.** *Neuron.* Mar 6;37(5):751-64.

Memberg SP, Hall AK. (1995) **Dividing neuron precursors express neuron-specific tubulin.** *J Neurobiol.* May;27(1):26-43.

Meyer G, Schaaps JP, Moreau L, Goffinet AM. (2000) **Embryonic and early fetal development of the human neocortex.** *J Neurosci.* Mar 1;20(5):1858-68.

Mihalas AB, Elsen GE, Bedogni F, Daza RAM, Ramos-Laguna KA, Arnold SJ, Hevner RF. (2016) **Intermediate Progenitor Cohorts Differentially Generate Cortical Layers and Require Tbr2 for Timely Acquisition of Neuronal Subtype Identity.** *Cell Rep.* Jun 28;16(1):92-105.

Miller FD, Gauthier AS. (2007) **Timing is everything: making neurons versus glia in the developing cortex.** *Neuron.* May 3;54(3):357-69.

Milosević NT, Ristanović D. (2007) **The Sholl analysis of neuronal cell images: semi-log or log-log method?** *J Theor Biol.* Mar 7;245(1):130-40.

Molyneaux BJ, Arlotta P, Menezes JR, Macklis JD. (2007) **Neuronal subtype specification in the cerebral cortex.** *Nat Rev Neurosci.* 2007 Jun;8(6):427-37.

Montiel JF, Vasistha NA, Garcia-Moreno F, Molnár Z. (2016) **From sauropsids to mammals and back: New approaches to comparative cortical development.** *J Comp Neurol.* Feb 15;524(3):630-45.

Nieto M, Schuurmans C, Britz O, Guillemot F. (2001) **Neural bHLH genes control the neuronal versus glial fate decision in cortical progenitors.** *Neuron.* Feb;29(2):401-13.

Noctor SC, Martínez-Cerdeño V, Ivic L, Kriegstein AR. (2004) **Cortical neurons arise in symmetric and asymmetric division zones and migrate through specific phases.** *Nat Neurosci.* Feb;7(2):136-44.

O'Leary DD, Chou SJ, Sahara S. (2007) **Area patterning of the mammalian cortex.** *Neuron.* Oct 25;56(2):252-69.

Oberst P, Fièvre S, Baumann N, Concetti C, Bartolini G, Jabaudon D. (2019) **Temporal plasticity of apical progenitors in the developing mouse neocortex.** *Nature.* Sep;573(7774):370-374.

Ono K, Takebayashi H, Ikenaka K. (2009) **Olig2 transcription factor in the developing and injured forebrain; cell lineage and glial development.** *Mol Cells.* Apr 30;27(4):397-401.

Ortega JA, Alcántara S. (2010) **BDNF/MAPK/ERK-induced BMP7 expression in the developing cerebral cortex induces premature radial glia differentiation and impairs neuronal migration.** *Cereb Cortex.* Sep;20(9):2132-44.

Pagin M, Pernebrink M, Giubbolini S, Barone C, Sambruni G, Zhu Y, Chiara M, Ottolenghi S, Pavesi G, Wei CL, Cantù C, Nicolis SK. (2021) **Sox2 controls neural stem cell self-renewal through a Fos-centered gene regulatory network.** *Stem Cells.* Aug;39(8):1107-1119.

Parthasarathy, S., Srivatsa, S., Nityanandam, A., & Tarabykin, V. (2014) **Ntf3 acts downstream of Sip1 in cortical postmitotic neurons to control progenitor cell fate through feedback signaling**. *Dev. Camb. Engl.,* 141, 3324 – 3330.

Parthasarathy S, Srivatsa S, Weber AI, Gräber N, Britanova OV, Borisova E, Bessa P, Ambrozkiewicz MC, Rosário M, Tarabykin V. (2021) **TrkC-T1, the Non-Catalytic Isoform of TrkC, Governs Neocortical Progenitor Fate Specification by Inhibition of MAP Kinase Signaling.** *Cereb Cortex.* Oct 22;31(12):5470-5486.

528 Paul V, Tonchev AB, Henningfeld KA, Pavlakis E, Rust B, Pieler T, Stoykova A. (2014) **Scratch2**
529 **modulates neurogenesis and cell migration through antagonism of bHLH proteins in**
530 **the developing neocortex.** *Cereb Cortex.* 2014 Mar;24(3):754-72.
531 Pieper, A., Rudolph, S., Wieser G.L., Götze, T., Mießner H., Yonemasu, T., Yan K., Tzvetanova, I.,
532 Castillo, B.D., Bode, U., Bormuth, I., Wadiche J.I., Schwab, M.H., & Goebbels, S. (2019)
533 **NeuroD2 controls inhibitory circuit formation in the molecular layer of the cerebel-**
534 **lum.** *Sci Rep.,* 5;9(1):1448.
535 Rakic P. **Mode of cell migration to the superficial layers of fetal monkey neocortex.** (1972) *J*
536 *Comp Neurol.* May;145(1):61-83.
537 Rakic P. (2009) **Evolution of the neocortex: a perspective from developmental biology.** *Nat Rev*
538 *Neurosci.* Oct;10(10):724-35.
539 Reyes JH, O'Shea KS, Wys NL, Velkey JM, Prieskorn DM, Wesolowski K, Miller JM, Altschuler
540 RA. (2008) **Glutamatergic neuronal differentiation of mouse embryonic stem cells after**
541 **transient expression of neurogenin 1 and treatment with BDNF and GDNF: in vitro**
542 **and in vivo studies.** *J Neurosci.* Nov 26;28(48):12622-31.
543 Sessa A, Ciabatti E, Drechsel D, Massimino L, Colasante G, Giannelli S, Satoh T, Akira S, Guil-
544 lemot F, Broccoli V. (2017) **The Tbr2 Molecular Network Controls Cortical Neuronal**
545 **Differentiation Through Complementary Genetic and Epigenetic Pathways.** *Cereb Cor-*
546 *tex*. Dec 1;27(12):5715.
547 Sessa A, Mao CA, Hadjantonakis AK, Klein WH, Broccoli V. (2008) **Tbr2 directs conversion of**
548 **radial glia into basal precursors and guides neuronal amplification by indirect neuro-**
549 **genesis in the developing neocortex.** *Neuron.* Oct 9;60(1):56-69.
550 Seuntjens E, Nityanandam A, Miquelajauregui A, Debruyn J, Stryjewska A, Goebbels S, Nave KA,
551 Huylebroeck D, Tarabykin V. (2009) **Sip1 regulates sequential fate decisions by feedback**
552 **signaling from postmitotic neurons to progenitors.** *Nat Neurosci.* Nov;12(11):1373-80.
553 Siegenthaler JA, Miller MW. (2005) **Transforming growth factor beta 1 promotes cell cycle exit**
554 **through the cyclin-dependent kinase inhibitor p21 in the developing cerebral cortex.** *J*
555 *Neurosci.* Sep 21;25(38):8627-36.
556 Sobecki M, Mrouj K, Camasses A, et al., Lafontaine DLj, Feil R, Fisher D. (2016) **The cell prolif-**
557 **eration antigen Ki-67 organises heterochromatin.** *Elife.* Mar 7;5:e13722.
558 Srivatsa, S., Parthasarathy, S., Britanova, O., Bormuth, I., Donahoo, A.-L., Ackerman, S.L.,
559 Richards, L.J., & Tarabykin, V. (2014) **Unc5C and DCC act downstream of Ctip2 and**

Satb2 and contribute to corpus callosum formation. *Nat. Commun.,* 5, 3708.

Subramanian L, Bershteyn M, Paredes MF, Kriegstein AR. (2017) **Dynamic behaviour of human neuroepithelial cells in the developing forebrain.** *Nat Commun.* Jan 31;8:14167.

Sugitani Y, Nakai S, Minowa O, Nishi M, Jishage K, Kawano H, Mori K, Ogawa M, Noda T. (2002) **Brn-1 and Brn-2 share crucial roles in the production and positioning of mouse neocortical neurons.** *Genes Dev.* Jul 15;16(14):1760-5.

Tarabykin V, Stoykova A, Usman N, Gruss P. (2001) **Cortical upper layer neurons derive from the subventricular zone as indicated by Svet1 gene expression.** *Development.* Jun;128(11):1983-93.

Taranova OV, Magness ST, Fagan BM, Wu Y, Surzenko N, Hutton SR, Pevny LH. (2006) **SOX2 is a dose-dependent regulator of retinal neural progenitor competence.** *Genes Dev.* May 1;20(9):1187-202.

Telley L, Govindan S, Prados J, Stevant I, Nef S, Dermitzakis E, Dayer A, Jabaudon D. (2016) **Sequential transcriptional waves direct the differentiation of newborn neurons in the mouse neocortex.** *Science.* Mar 25;351(6280):1443-6.

Tissir F, Goffinet AM. (2003) **Reelin and brain development.** *Nat Rev Neurosci.* Jun;4(6):496-505.

Tutukova S, Tarabykin V, Hermandez-M LR. (2021) **The Role of Neurod Genes in Brain Development, Function and Disease.** *Front. Mol. Neurosci.* 14: 662774.

Wilsch-Bräuninger M, Florio M, Huttner WB. (2016) **Neocortex expansion in development and evolution - from cell biology to single genes.** *Curr Opin Neurobiol.* Aug;39:122-32.

Wu SX, Goebbels S, Nakamura K, Nakamura K, Kometani K, Minato N, Kaneko T, Nave KA, Tamamaki N. (2005). **Pyramidal neurons of upper cortical layers generated by NEX-positive progenitor cells in the subventricular zone.** *Proc Natl Acad Sci U S A.* Nov 22;102(47):17172-7.

Xing L, Larsen RS, Bjorklund GR, Li X, Wu Y, Philpot BD, Snider WD, Newbern JM. (2016) **Layer specific and general requirements for ERK/MAPK signaling in the developing neocortex.** *Elife.* Feb 5;5:e11123.

Yan K, Bormuth I, Bormuth O, Tutukova S, Renner A, Bessa P, Schaub T, Rosário M, Tarabykin V. (2023) **TrkB-dependent EphrinA reverse signaling regulates callosal axon fasciculate growth downstream of Neurod2/6.** *Cereb Cortex.* Feb 20;33(5):1752-1767.

Figures and captions

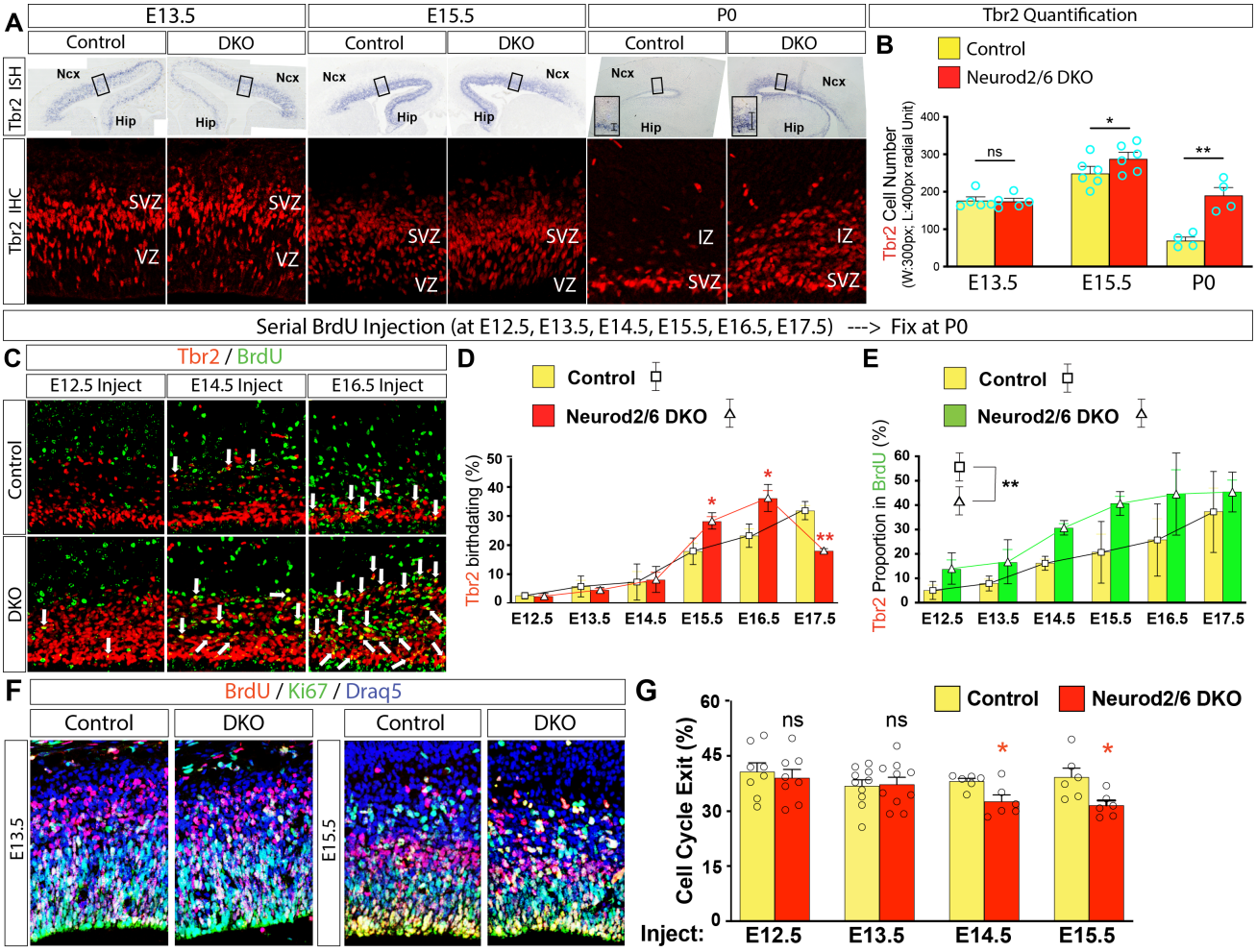

Figure 1 Tbr2+ basal progenitors are ectopically upregulated in Neurod2/6 DKO brains.

(A, B) *In situ* hybridization (ISH, upper panel) and IF (lower panel) for Tbr2 on control and DKO brain sections at the age of E13.5, E15.5 and P0 shows the progressive emergence of ectopic Tbr2+ basal progenitors (BPs) in the IZ of DKO brains (**A**). (**B**) Cell quantification shows the number of Tbr2+ cells in DKO brains is similar with that of control at E13.5 ($p = 0.87$, ns; n = 5), and is mildly elevated by 15.92% ± 8.49% at E15.5 ($p = 0.029$, *; n = 6). Notably, the number of Tbr2+ cells in DKO brains is increased by 1.73 ± 0.33 folds than that of control at P0 ($p = 0.0023$, **; n = 4).

(C-E) Mouse brains carrying BrdU injected at serial stages of cortical neurogenesis (E12.5 to E17.5) were fixed at P0 and analyzed by IF for BrdU and Tbr2. Each arrowhead indicates one or one cluster of BrdU/Tbr2 double positive cells (**C**). (**D**) Birthdating analysis for Tbr2+ cells by proportional quantification in control and DKO brains at

P0. The production of Tbr2+ cells at P0 displays progressively proportional increment along developmental timing in control brains, however, the proportion of Tbr2+ cell production is substantially elevated at E15.5 ($p = 0.029$, *; n = 3) and E16.5 ($p = 0.022$, *; n = 3), but steeply reduced at E17.5 ($p = 0.0017$, **; n = 3) in DKO brains. Two-way *Anova* analysis is not applied in this scenario because of the existing phenotypes and different denominators. (**E**) Proportional quantification of BrdU/Tbr2 double positive cells relative to total BrdU+ cells in all cortical layers analyzed by two-way *Anova* statistics. There is a significantly larger proportion of BrdU+/Tbr2+ cells accumulated in the SVZ/IZ of DKO brains (F(DFn, DFd) = F(5, 10) = 5.59, $p = 0.0086$, **; each stage n = 3).

(F, G) Cell cycle exit analysis at serial developmental stages of corticogenesis (BrdU injected at E12.5 to E15.5). The control and DKO brains were fixed 24 hours after BrdU injection and analyzed by IF for BrdU and Ki67 (Draq5 nuclei staining as counter staining, **F**). The proportions of progenitors quitting cell cycles after one day are counted as the numbers of BrdU+/Ki67- cells relative to total BrdU+ cell numbers (**G**). The progenitor proportions exiting cell cycles in DKO cortices are similar with those of controls at E12.5 ($p = 0.62$, ns; n = 8) and E13.5 ($p = 0.87$, ns; n = 10), however, the proportions are significantly reduced in DKO brains in comparison to those of control brains at E14.5 (by 14.48% ± 5.10%, $p = 0.018$, *; n = 6) and E15.5 (by 19.55% ± 7.11%, $p = 0.021$, *; n = 6).

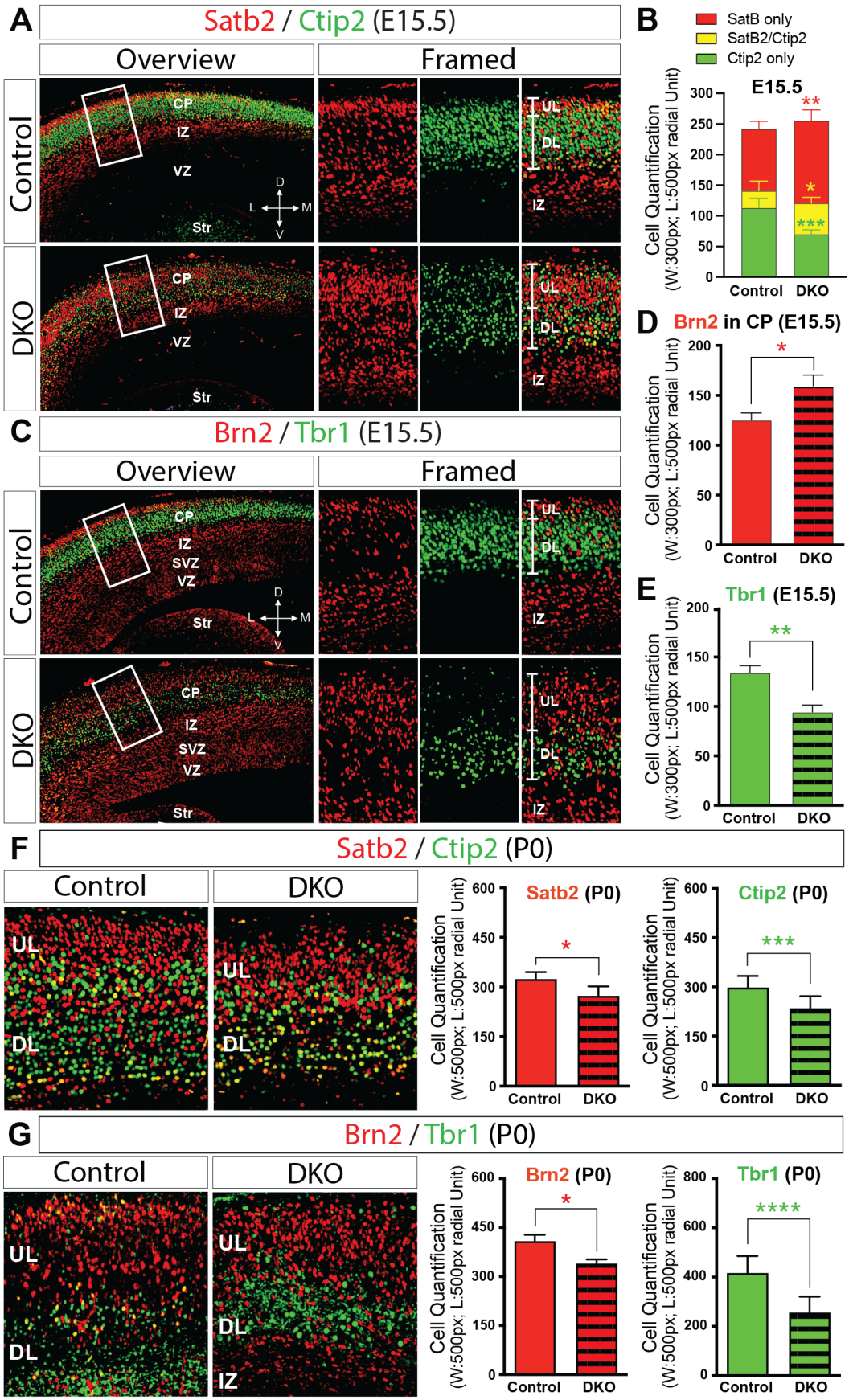
A
Satb2 / Ctip2 (E15.5)
Overview
Framed
Control
DKO
CP
IZ
VZ
Str
UL
DL
B
SatB only
SatB2/Ctip2
Ctip2 only
E15.5
Cell Quantification
(W:300px; L:500px radial Unit)
Control
DKO
C
Brn2 / Tbr1 (E15.5)
SVZ
D
Brn2 in CP (E15.5)
E
Tbr1 (E15.5)
F
Satb2 / Ctip2 (P0)
Satb2 (P0)
Ctip2 (P0)
(W:500px; L:500px radial Unit)
G
Brn2 / Tbr1 (P0)
Brn2 (P0)
Tbr1 (P0)

624

Figure 2 Cortical cell fate is misprogrammed in Neurod2/6 double deficient mice.

(A, B) Immunofluorescence staining (IF, A) for Satb2 and Ctip2 on coronal sections of control and Neurod2/6 double deficient (DKO) brains shows increased Satb2+ upper layer neurons (UL, red) and decreased Ctip2+ deeper layer neurons (DL, green) in DKO brains at E15.5. (B) Cell quantification shows the number of single Satb2+ UL cells in DKO brains (134.90 ± 7.93, n = 5) is increased by 25.11% ± 7.18% (p = 0.0081, **) relative to that of control brains (101.00 ± 5.56, n = 5), nevertheless, the number of single Ctip2+ DL cells in DKO brains (69.80 ± 3.25, n = 5) is decreased by 38.20% ± 6.89% (p = 0.00050, ***) relative to that of control brains (112.90 ± 7.07, n = 5). Moreover, the number of Satb2/Ctip2 double positive cells in DKO brains (50.80 ± 4.34) is also increased by 81.43% ± 29.81% (p = 0.026, *) in comparison to that of control brains (28.00 ± 7.13). **CP**, cortical plate; **IZ**, intermediate zone; **VZ**, ventricular zone; **Str**, striatum. **D**, dorsal; **L**, lateral; **V**, ventral; **M**, medial.

(**C-E**) IF for Brn2 and Tbr1 at E15.5 also shows increased Brn2+ UL cells (red) and decreased Tbr1+ DL cells (green) in DKO brains. The number of Brn2+ UL cells in DKO brains (159.50 ± 10.96, n = 5) is increased by 27.17% ± 10.35% (p = 0.030, *) relative to that of control brains (125.40 ± 6.94, n = 5), while the number of Tbr1+ DL cells in DKO brains (94.47 ± 15.53, n = 5) is decreased by 29.50% ± 7.39% (p = 0.0040, **) relative to that of control brains (134.00 ± 15.78, n = 5). **SVZ**, subventricular zone.

(F, G) IF for Satb2/Ctip2 (F) and Brn2/Tbr1 (G) on coronal sections of control and DKO brains shows both UL and DL cells are reduced in DKO brains at P0. The Satb2+ UL and Ctip2+ DL cells are decreased by 15.61% ± 11.07% (p = 0.041, *; n = 8) and 21.31% ± 17.17% (p = 0.00080, ***; n = 8), respectively. Moreover, the Brn2+ UL and Tbr1+ DL cells are decreased by 16.82% ± 5.78% (p = 0.011, *; n = 6) and 38.68% ± 22.64% (p < 0.0001, ****; n = 6), respectively.

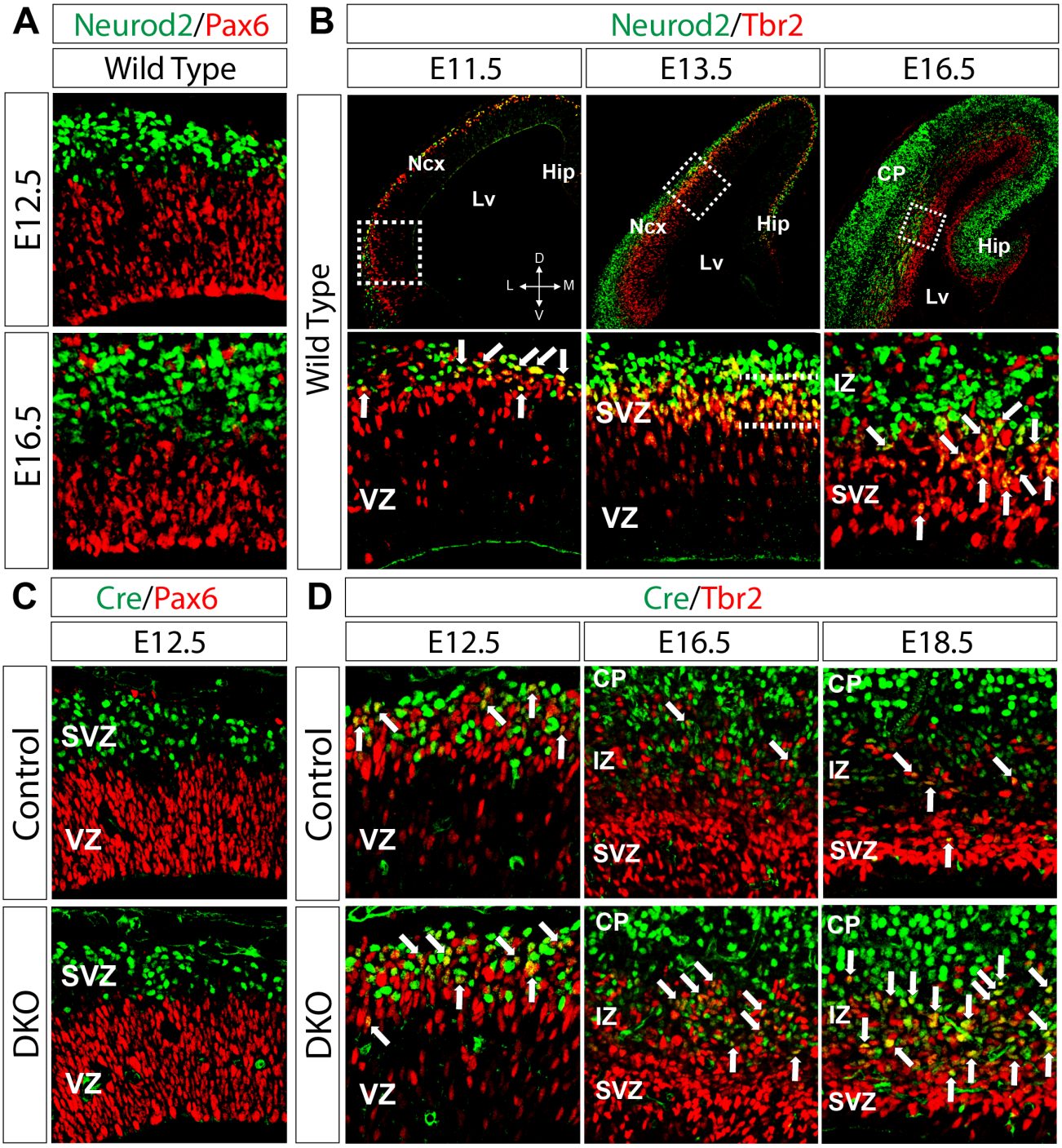

Figure 3 Neurod2/6 are transiently expressed in Tbr2+ basal progenitors.

(A) IF for Neurod2 (green) and Pax6 (red) on wild type brain sections at E12.5 and E16.5 shows that Neurod2 is barely expressed in Pax6+ apical progenitors (APs).

(B) IF for Neurod2 and Tbr2 (red) on wild type brain sections at E11.5, E13.5 and E16.5 shows that a subpopulation of Tbr2+ BPs in the SVZ during corticogenesis also express Neurod2. The images in lower panel represent the magnified views of framed parts in upper panel.

(C) IF for Cre (Neurod6, green) and Pax6 on coronal sections of control and DKO brains at E12.5 shows that Neurod6 is never present in Pax6+ APs.

(D) IF for Cre and Tbr2 on control and DKO brain sections at E12.5, E16.5 and E18.5 shows that Neurod6 is transiently expressed in Tbr2+ BPs throughout cortical neurogenesis in control brains (upper panel), and that Cre/Tbr2 double positive cells are accumulating during development in DKO brains (lower panel).

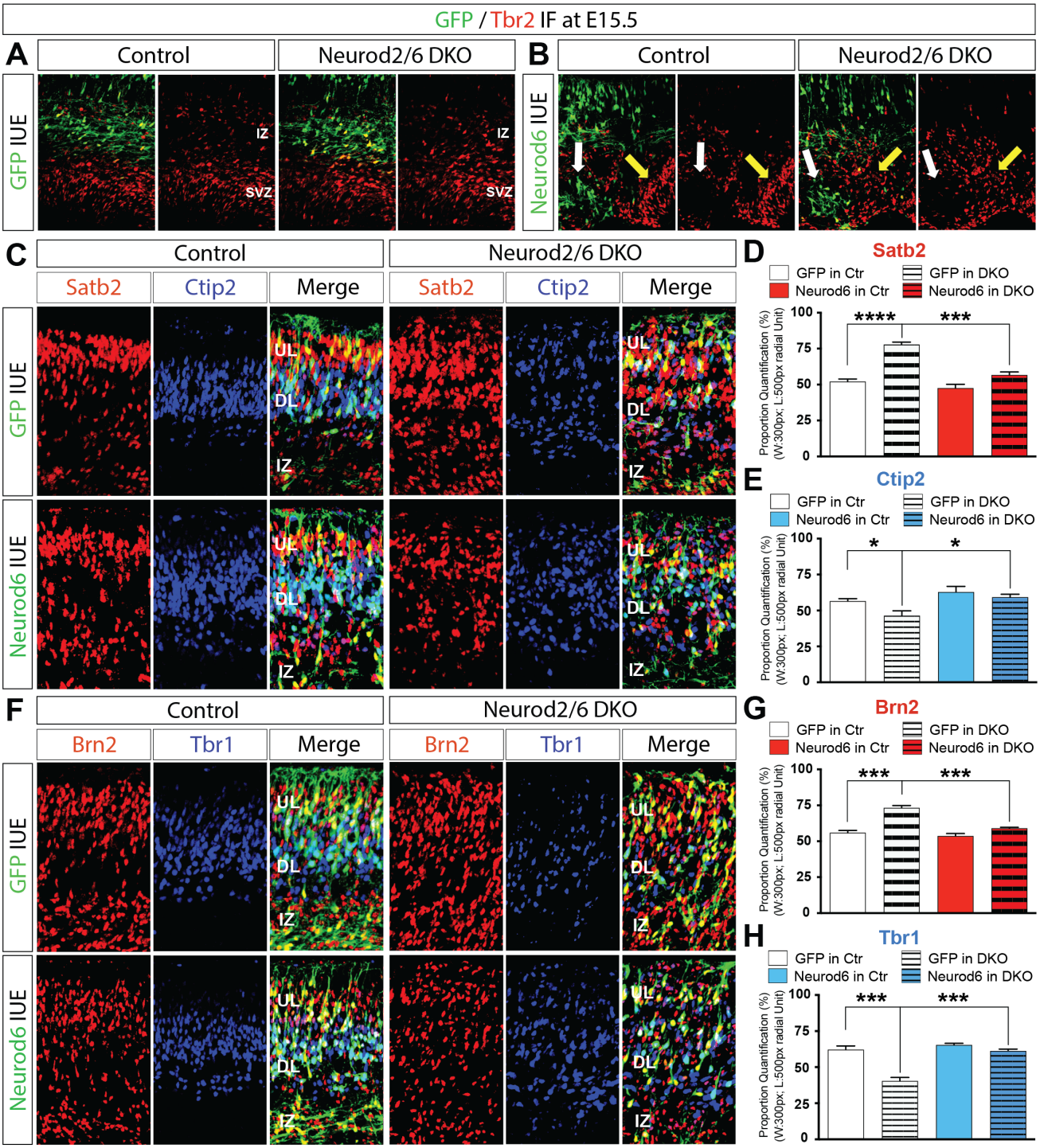

Figure 4 Restoration of Neurod6 expression in DKO cortices at an earlier neurogenic stage rescues cell specification deficits.

(A, B) GFP or bicistronic Neurod6-GFP was electroporated into control and DKO brains at E12.5, which were then sampled at E15.5 (the same in **C - H**). IF for GFP and Tbr2 on GFP- or Neurod6-electroporated brain sections shows that Neurod6 over-expression

671 in both control and DKO brains causes depletion of Tbr2+ BPs at IUE sites (white
672 arrowheads) but not in neighboring non-IUE regions (yellow arrowheads, **B**), while
673 GFP IUE does not disturb the distribution of Tbr2+ BPs (**A**).

674 **(C-E)** IF for GFP, Satb2 and Ctip2 on GFP- or Neurod6-electroporated brain sections (at
675 E15.5) shows in utero electroporation (IUE) of Neurod6 in DKO brains downregulates
676 UL neurons but upregulates DL neurons (**C**). Proportional quantification of Satb2/GFP
677 (**D**) or Ctip2/GFP (**E**) double positive cells relative to all GFP+ cells shows the ratio
678 of Satb2/GFP+ UL cells in GFP-electroporated DKO brains is 77.90% ± 3.22% (n =
679 4) in comparison to GFP-electroporated control brains (52.11% ± 3.47%, n = 4), but
680 Neurod6 IUE reduced the ratio to 56.65% ± 4.11% (p = 0.00019, ***; n = 4). On the
681 other hand, the ratio of Ctip2/GFP+ DL cells in GFP-electroporated DKO brains is
682 46.44% ± 6.67% (n = 4) in comparison to GFP-electroporated control brains (56.62%
683 ± 3.21%, n = 4), whereas the ratio is elevated to 59.32% ± 3.92% (p = 0.016, *; n = 4)
684 when Neurod6 was electroporated in DKO brains.

685 **(F-H)** IF for GFP, Brn2 and Tbr1 on GFP- or Neurod6-electroporated brain sections con-
686 firms the rescue effects of Neurod6 IUE in DKO brains (**F**). The ratio of Brn2/GFP+
687 UL cells in GFP-electroporated DKO brains is 73.29% ± 3.11% (n = 4) in compari-
688 son to GFP-electroporated control brains (55.97% ± 3.12%, n = 4), however, Neu-
689 rod6 IUE reduced the ratio to 59.03% ± 1.40% (p = 0.00020, ***; n = 4) (**G**). The
690 ratio of Tbr1/GFP+ DL cells in GFP-electroporated DKO brains is 40.45% ± 4.89%
691 (n = 4) in comparison to GFP-electroporated control brains (62.18% ± 5.02%, n = 4),
692 but Neurod6 restoration in DKO brains elevated the ratio up to 61.33% ± 2.40% (p =
693 0.00029, ***; n = 4) (**H**).

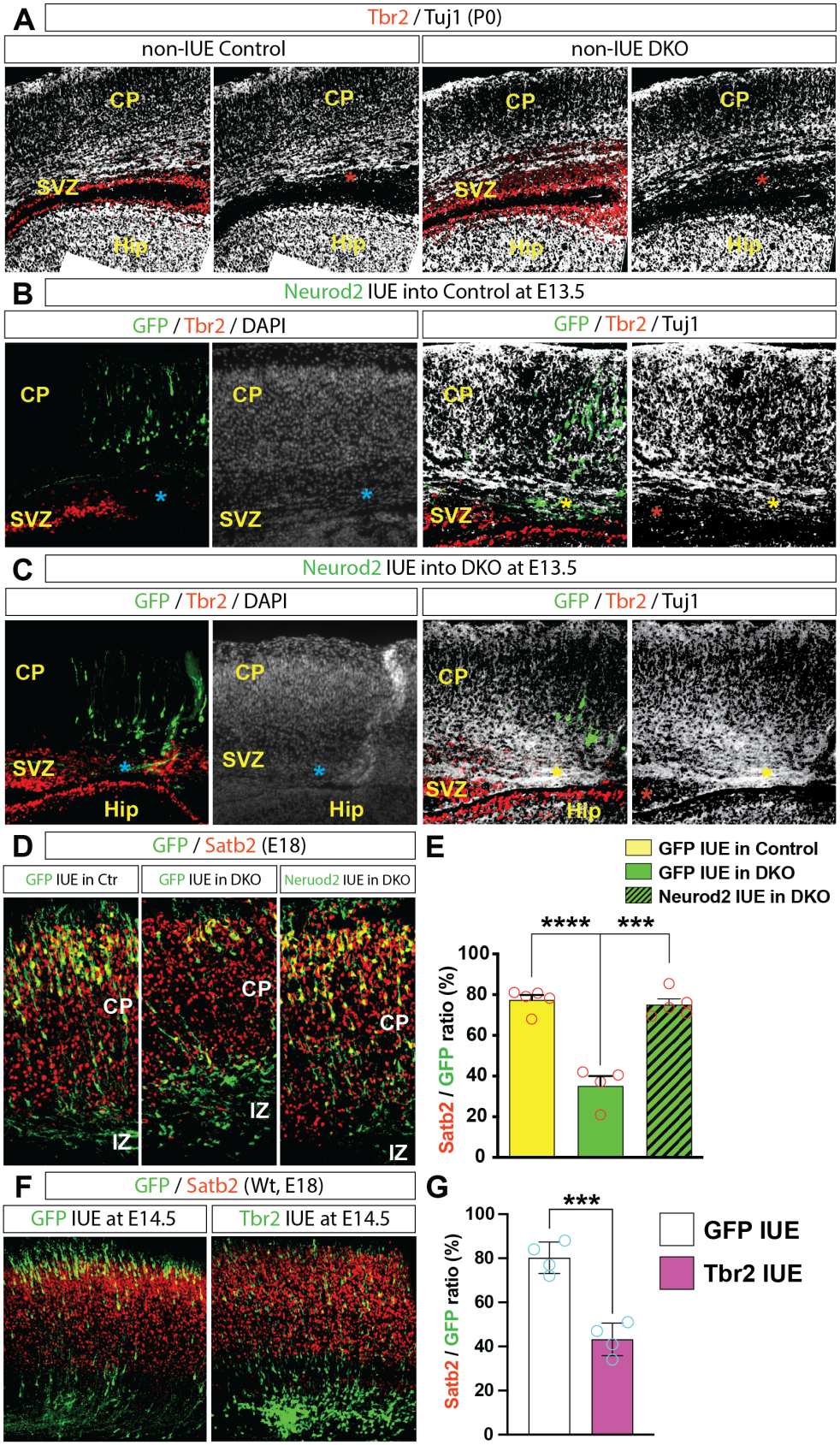
A
Tbr2 / Tuj1 (P0)
non-IUE Control
non-IUE DKO
CP
SVZ
Hip
B
Neurod2 IUE into Control at E13.5
GFP / Tbr2 / DAPI
GFP / Tbr2 / Tuj1
C
Neurod2 IUE into DKO at E13.5
D
GFP / Satb2 (E18)
GFP IUE in Ctr
GFP IUE in DKO
Neruod2 IUE in DKO
IZ
E
GFP IUE in Control
GFP IUE in DKO
Neurod2 IUE in DKO
****
***
Satb2 / GFP ratio (%)
F
GFP / Satb2 (Wt, E18)
GFP IUE at E14.5
Tbr2 IUE at E14.5
G
GFP IUE
Tbr2 IUE

694

695 **Figure 5 Electroporated Neurod2 at a later neurogenic stage instructs basal progenitor differ-**
696 **entiation into upper layer neurons.**

697 **(A)** IF for Tbr2 and Tuj1 on control and DKO brain sections at P0 shows that Tuj1 expres-
698 sion is extremely weak in the SVZ enriched with Tbr2+ BPs (red asterisks).

699 **(B, C)** Bicistronic Neurod2-GFP was electroporated into control (**B**) and DKO (**C**) brains at
700 E13.5, which were sampled at E18.5 (the same in **D, E**). IF for GFP, Tbr2 and Tuj1 on
701 Neurod2-electroporated brain sections shows that IUE of Neurod2 in both control and
702 DKO brains results in onset of Tuj1 expression in Tbr2+ BPs at IUE sites (blue aster-
703 isks) but not in adjacent SVZ. DAPI nuclei counterstaining on the neighboring sections
704 shows that there are cell populations at IUE sites to avoid an artifact caused by IUE.
705 These cells at IUE sites instead express Tuj1, an earliest neurogenic marker (yellow
706 asterisks), but not Tbr2, in contrast to neighboring Tbr2+ cells in SVZ (red asterisks).

707 **(D, E)** GFP and bicistronic Neurod2-GFP was electroporated into control and DKO brains at
708 E14.5, which were then sampled at E18.5. IF for GFP and Satb2 shows that the pro-
709 portion of GFP+/Satb2+ relative to all GFP-electroporated cells in DKO brains
710 (~35.18%, n = 4) is significantly reduced in comparison to that in control brains
711 (~77.48%, n = 5) ($p < 0.0001$, ****). IUE of Neurod2 into DKO brains promotes
712 Satb2+ cell differentiation and increases the ratio up to ~75.11% ($p = 0.00010$, ***; n
713 = 5), similar to control brains.

714 **(F, G)** GFP and bicistronic Tbr2-GFP was electroporated into wild type brains at E14.5,
715 which were then sampled at E18.5. IF for GFP and Satb2 shows that Tbr2 IUE restricts
716 the majority of cells beneath CP, resulting in reduced ratio of Satb2+ UL cells by 46.11%
717 ± 6.41% ($p = 0.00040$, ***; n = 4) relative to total GFP+ cells in comparison to that of
718 GFP-electroporated controls.

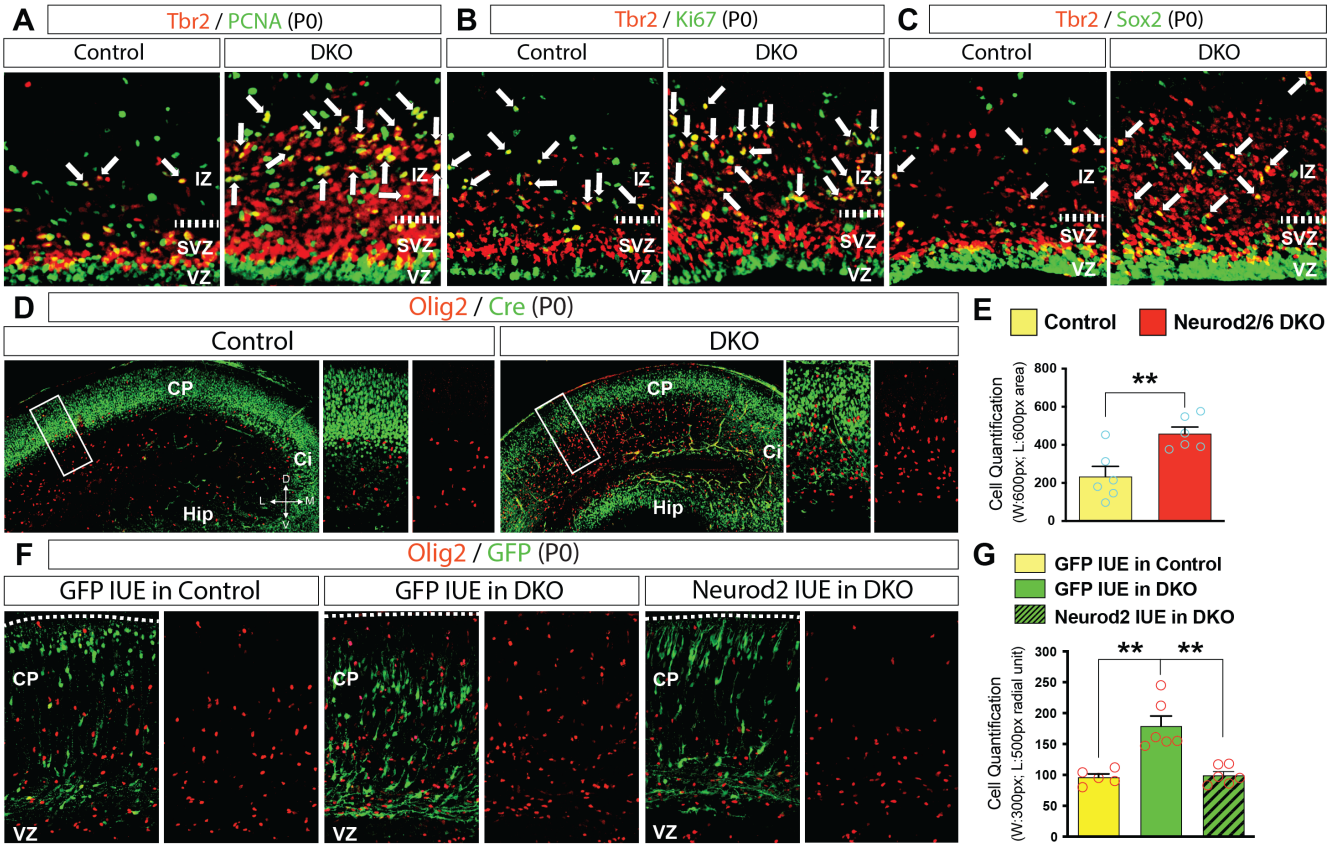

Figure 6 Olig2+ glial progenitors are ectopically elevated in Neurod2/6 DKO brains

(A-C) Co-IF for Tbr2/PCNA (**A**), Tbr2/Ki67 (**B**) and Tbr2/Sox2 (**C**) on control and DKO cerebral coronal sections at E18.5 shows that a large subpopulation of ectopic Tbr2+ cells co-express PCNA, Ki67 and Sox2 in the IZ of DKO brains. Each arrowhead indicates one or one cluster of double positive cells in the IZ.

(D, E) IF for Cre (green) and Olig2 (red) on control and DKO cerebral coronal sections at P0 (**D**). (**E**) Quantification of Olig2+ glial progenitors for control and DKO cortices at P0. The number of Olig2+ cells in DKO brains is upregulated to 458.80 ± 34.89 (p = 0.0053, **; n = 6) in contrast to that of controls (233.80 ± 52.92, n = 6).

(F, G) GFP or bicistronic Neurod2-GFP was electroporated into control and DKO brains at E14.5, which were later sampled at P0. IF for GFP (green) and Olig2 (red) on GFP- or Neurod2-electroporated brain sections shows the Olig2+ cells in GFP-electroporated region of DKO brains are upregulated in comparison to GFP-electroporated control brains, which is normalized by Neurod2 IUE in DKO brains (**F**). (**G**) Quantification of Olig2+ cells in the GFP+ regions of GFP or Neurod2-GFP electroporated control

and DKO brains shows that the number of Olig2+ cells in GFP-electroporated DKO brain areas is 179.00 ± 39.98 (p = 0.0017, **; n = 6) in contrast to that of GFP-electroporated control brain areas (96.20 ± 12.38, n = 5), however, the number in Neurod2-electroporated DKO brain areas is reduced to 99.33 ± 15.03 (p = 0.0010, **; n = 6).